ELSEVIER

Journal of Hydrology 257 (2002) 42–58

Journal of Hydrology

www.elsevier.com/locate/jhydrol

Comparison of turbulence models for stage-discharge rating curve prediction in reach-scale compound channel flows using two-dimensional finite element methods

C.A.M.E. Wilson[a,*], P.D. Bates[b], J.-M. Hervouet[c]

[a]*Environmental Water Management Research Centre, Cardiff School of Engineering, Cardiff University, Cardiff, Wales CF24 3TB, UK*
[b]*School of Geographical Sciences, University of Bristol, Clifton, Bristol BS8 1SS, UK*
[c]*Department Laboratoire National d'Hydraulique, EDF Chatou, Paris, France*

Received 21 February 2001; revised 1 August 2001; accepted 27 September 2001

Abstract

This paper attempts to assess the accuracy of constant eddy viscosity, Elder and $k-\epsilon$ turbulence models in the numerical simulation of reach-scale compound channel flows using two-dimensional (2D) finite element methods. Assessment was conducted using benchmark stage-discharge data collected from straight and meandering compound channel configurations at the UK Engineering and Physical Science Research Council (EPSRC) Flood Channel Facility. For mesh resolutions and topologies used in reach-scale studies, all models were found to be adequate predictors (<5% error in predicted flow depth) of the stage-discharge relationship at moderate overbank flows (Figs. 1 and 2). However, at inbank and low overbank flows the Elder and $k-\epsilon$ turbulence models can reproduce stage-discharge points with much greater accuracy than the constant eddy viscosity model. Hence, for an unsteady simulation where low flows are relevant a constant eddy viscosity turbulence closure may prove problematic. In terms of computed lateral distributions of depth-averaged velocity for both channel configurations, at higher depths (Relative depth = 0.666) all turbulence models predict the velocity with greater accuracy than at a lower depth (Relative depth = 0.333). At this latter depth, all turbulence models predict the depth-averaged longitudinal velocity distribution with poor accuracy (>20% error). Also, sensitivity of the turbulence parameter calibration with respect to the predicted flow depth showed that the constant eddy viscosity model's performance can be highly dependent on the choice of turbulence parameter value.

Keywords: Hydrodynamics; Numerical model; Flood routing; Compound channel flow

1. Introduction

An accurate assessment of the stage-discharge relationship is fundamental for flood management and in the design of waterways. There are many methods for determining the conveyance capacity and the extent of flood inundation, and these generally fall into two categories: empirical and numerical approaches. A number of researchers have proposed empirical methods, primarily based on data from small and large flumes that contain regularly meandering compound channels (Wark et al., 1994; Shiono et al., 1999; Greenhill and Sellin, 1993). However for practical use, a prediction method that can be applied generically to natural rivers needs to be developed. Also, these empirical methods typically use a one-dimensional (1D) approach based on a reach-averaged

* Corresponding author.
E-mail address: wilsonca@cardiff.ac.uk (C.A.M.E. Wilson).

0022-1694/02/$ - see front matter
PII: S0022-1694(01)00553-4

Nomenclature

c_μ, $c_{1\epsilon}$, $c_{2\epsilon}$	coefficients in the $k-\epsilon$ equations
DR	relative depth (DR $= h_f/y_{bk}$)
E_x, E_y	longitudinal and transverse diffusion coefficients
F_x, F_y	source terms to account for boundary friction
g	gravitational acceleration
h	flow depth
h_f	overbank flow depth
k	turbulent kinetic energy
P	production of kinetic turbulent energy
t	time
u	depth-averaged streamwise velocity
u_i	velocity vector
u_*	shear velocity
v	depth-averaged cross-streamwise velocity
v_T	turbulent eddy viscosity
y_{bf}	bankfull flow depth
z	elevation
α_x	longitudinal dimensionless dispersion coefficient used by Elder
α_y	transverse dimensionless dispersion coefficient used by Elder
β	depth-averaged resultant dimensionless dispersion coefficient
ϵ	turbulent dissipation
θ	local boundary slope
ρ	density of water

cross-section under steady state conditions, whereas a method which can predict the stage-discharge curve at sections along a reach for both steady state and during the advancement of a flood wave is often needed. The form of the stage-discharge curve will be highly dependent on the main channel and floodplain geometric properties including the meander belt width to floodway width ratio, and main channel and floodplain meander wavelength. Such relationships may be quite complex and there is a limit to the extent to which empirical methods can inform researchers of these.

For numerical approaches, flow boundary conditions are specified at the upstream and downstream ends of a river reach and flow conditions at an individual internal cross-section are calculated directly by the model on the basis of its flood routing properties. A validated model capable of predicting a reach stage-discharge curve on the basis of available gauging data collected at some distance from the site of interest would be of major benefit to practicing hydrologists. The development of computational fluid dynamics (CFD) for hydraulic applications over the last decade now provides the necessary technology to accomplish this task.

At present, consulting engineers use 1D numerical models to solve most river hydraulic routing problems (Samuel, 1985). However not all problems can be solved by a 1D approach. Large-scale flume experiments in the EPSRC Flood Channel Facility (FCF) have shown that when water inundates the floodplain the resulting flows are three-dimensional (3D). In open channel flow irrespective of whether a one, two or three-dimensional approach is taken, the governing equations originate from the Reynolds averaged Navier–Stokes equations. There are many approaches to turbulence modeling for this equation system from using a dispersion term in 1D models to using more advanced approaches such as the two-equation linear $k-\epsilon$ model in higher dimensional models. As the dimensionality of numerical representation increases, the manner in which

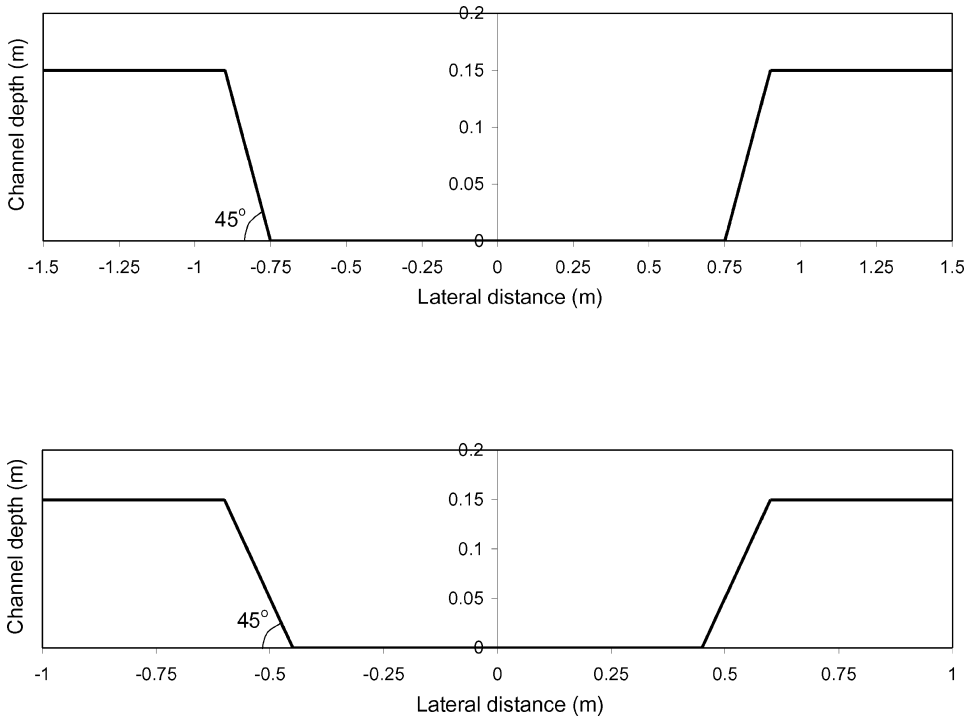

Fig. 1. Main channel cross-sectional details of the EPSRC FCF at a distorted scale (a) series A straight channel (b) series B meandering channel.

turbulence can be represented changes. In applications with complex flow structure and strong velocity gradients in depth, transverse and longitudinal directions, it is likely that the turbulence will be anisotropic and it becomes necessary to use a more accurate representation of turbulence. However, whilst two-dimensional (2D) modelling may allow use of more sophisticated turbulence closures to be employed relative to 1D approaches, the degree of turbulence model complexity necessary to adequately reproduce stage-discharge curves is as yet unknown. This paper attempts to resolve this question by comparing both stage-discharge predictions, and depth-averaged velocity predictions of three turbulence models, against high quality data from two FCF compound channel configurations which have differing degrees of turbulence intensity.

At present, the most developed and widely used turbulence models, and hence those which might be used for engineering applications, are the zero-equation and two equation models. Most commercial codes include one or both of these schemes. Higher order approaches such as the Reynolds stress equation (RSM), algebraic stress and large eddy simulation (LES) models are at present only at the research and development stage within hydraulic engineering, see Naot et al. (1993), Lin and Shiono (1995) and Cokljat and Kralj (1997). Hence this paper will focus on the simpler turbulence schemes incorporated within 2D models, taking the view that these may have the greatest potential as practical engineering tools.

Turbulence model performance is also strongly linked to mesh resolution as this fundamentally limits the eddy sizes and velocity gradients that can be resolved. For reach-scale applications, model extent is determined by the spacing of available gauging stations that is primarily defined by their flood-warning role. In the UK and the US, gauges are of the order of 10–40 km apart. Even with a 2D model, such reach lengths are at the limit of our current computational ability for practical applications and necessitate compromises over mesh resolution in

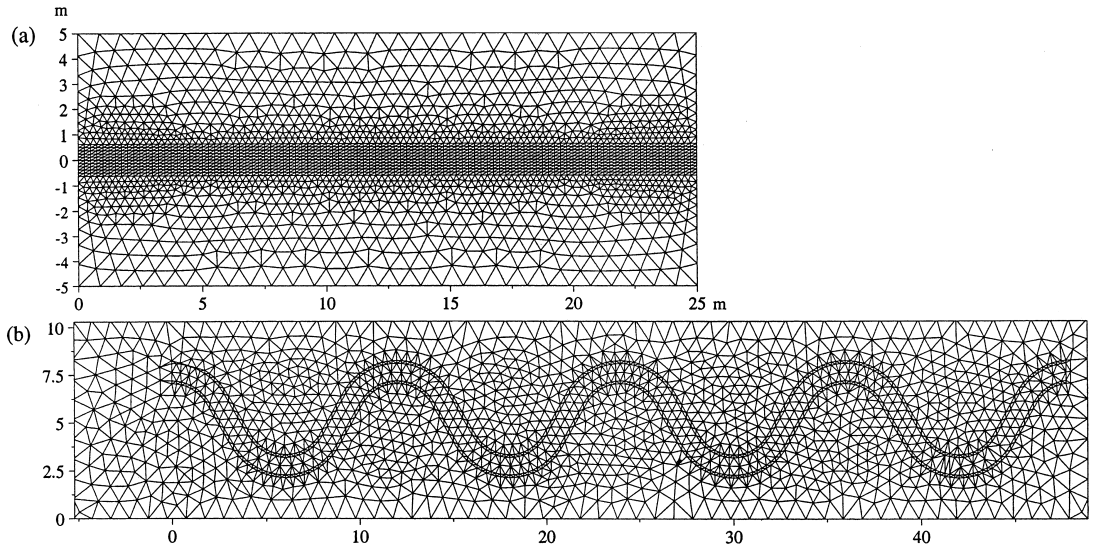

Fig. 2. Finite element meshes developed for the: (a) EPSRC FCF series A channel with trapezoidal cross-section; (b) EPSRC FCF series B channel with trapezoidal cross-section.

order to achieve an efficient model. Hence, a subsidiary aim of the research reported here was to test the effect of these compromises upon predicted stage-discharge curves and depth-averaged velocities in reach-scale applications. This goes beyond traditional concerns relating to the impact of mesh resolution on numerical accuracy and begins to force consideration of resolution impacts on process representation. Whilst a full analysis of these effects is beyond the scope of this paper, such studies may become increasingly necessary in the future.

Thus, this paper has three main objectives. First, it seeks to determine the degree of complexity with which turbulence needs to be represented in order to reproduce the stage-discharge curve to an acceptable accuracy along a compound channel reach, using a 2D flood routing model with a typical reach-scale discretization. Second, this analysis is extended to examine the effects of turbulence model choice upon the lateral distribution of depth-averaged velocity. Third, the paper compares the calibration with respect to turbulence parameters for the zero-equation model and assesses the sensitivity of turbulent eddy viscosity values for stage-discharge prediction.

2. Research design

Commercial depth-averaged codes have a variety of turbulence models. The simplest approach is the zero-equation model. This uses either a constant eddy viscosity model or a model where an algebraic expression is used to calculate the turbulent eddy viscosity or turbulent diffusivity as a function of water depth, and this parameter is calculated at every node within the domain. Both variants require the input of turbulence parameters: the former needs a turbulent eddy viscosity and the latter requires one or more dimensionless dispersion coefficients. A more advanced approach is the two-equation model which, rather than requiring the pre-specification of coefficients, has accepted coefficients for open channel flow applications. Thus, no input of turbulence parameters and hence no calibration with respect to turbulence is required. Although the $k-\epsilon$ model is a definite advance on the constant eddy viscosity model it is still limited in that it assumes that turbulence is isotropic. Experimental measurements in a flume with simple cross-sectional shape have shown that this is not the case (Miller, 1971; Keefer, 1971) and the structure of secondary flow and the associated turbulence intensities have been found to be highly

Table 1
Hydraulic parameters for the straight and meandering experiments

Test ref	Configuration	Discharge ($m^3 s^{-1}$)	Main channel flow depth (m)
A1	Straight channel, straight floodplain boundaries	0.0279	0.0467
		0.0614	0.0753
		0.1053	0.1
		0.2022	0.1502
		0.2857	0.1755
		0.3325	0.198
		0.5024	0.2391
		0.6345	0.2639
		0.8851	0.3069
B21	Meandering channel (sinuosity = 1.34) with straight floodplain boundaries	0.01975	0.059
		0.03056	0.077
		0.04708	0.102
		0.0824	0.164
		0.1494	0.182
		0.30228	0.208

directional. Furthermore, in a channel with complex cross-section the transverse and longitudinal diffusivity has been found to be variable between the main channel and floodplain zones (Arnold et al., 1989; Alavian and Chu, 1985). A possible solution is to use an anisotropic turbulence closure such as the one equation Elder scheme (Fischer et al., 1979). This is somewhat simpler than the k–ϵ turbulence model but allows separate dimensionless dispersion coefficients to be specified in the longitudinal and transverse directions. This representation may be particularly relevant to compound channel flow where the lateral gradient in longitudinal velocity causes the formation of a turbulent shear mixing region at the main channel–floodplain interface.

The validation and development of numerical models has been hindered by the lack of available and reliable field data consisting of both hydraulic and topographic information. This has presented calibration problems in that there can be insufficient data to carry out calibration and validation independently from each other. This research deals with this issue by assessing the predictive ability of each turbulence model using data from the EPSRC FCF. The FCF is a 60 m long, 10 m wide scaled physical model that provides a large scale facility to enable fully turbulent flow regimes to develop. Scaling provides the basis for high quality data collection in fully controlled conditions. A fuller description can be found in Shiono and Knight (1991). Error analysis conducted on the physical model data showed that flow depth and discharge measurement were to an accuracy of 1 and 2%, respectively, (Greenhill, 1992). The experiments used for the simulations presented in this paper are given in Table 1 and cross-sections are given in Fig. 1a and b.

In the series A phase, experiments were conducted in a straight compound channel. In the series B phase, experiments were conducted in a meandering main channel with two sinuosities, both with a straight floodplain boundary. In a straight compound channel the dominant flow mechanism which incurs energy loss other than that due to skin friction, is the interaction between the main channel and floodplain flows which results in a transfer of momentum between these zones. A region of turbulent shear forms, consisting of a bank of vortices with vertically aligned axes along the main channel and floodplain interface (Sellin, 1961). In a meandering compound channel, the turbulent mixing processes are more complex. The flow mechanisms which are responsible can be identified as the following: curvature-induced secondary currents, horizontal shearing, the expansion and contraction of floodplain flow and the outer meander belt floodplain flow dominance (Willetts and Hardwick, 1993; Shiono and Muto, 1998; Wilson, 1999; Knight, 1999) and these are described briefly below. For overbank flow the bend apex induces a secondary cell that rotates in the opposite direction to those of inbank flow. The flow within the main channel tends to follow the local channel direction while the floodplain flow generally follows a longitudinal direction

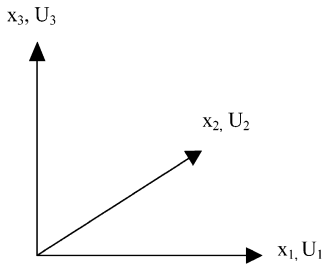

Fig. 3. Definition of cartesian tensor notation.

parallel to the floodplain boundaries. Thus the floodplain flow passes over the main channel and induces a horizontal shear layer. The horizontal shear layer develops over the cross-over region, and at the apex reaches a minimum value where the channels are co-flowing and a maximum at the cross-over region. At the cross-over region, the floodplain flow experiences a sudden expansion followed by a sudden contraction, this is where the flow plunges into the deeper main channel and then is ejected onto the adjacent downstream floodplain. There is a condition at which the additional flow resistance induced by the meandering main channel has no impedance on the outer meander belt floodplain flow. This depends both on the meander belt width to floodplain width ratio and the main channel sinuosity. The straight (phase A) and meandering (phase B) channel configurations have distinctly different flow systems and degrees of turbulence intensity (Knight and Shiono, 1990), providing a good basis for the comparison of turbulence models.

The exact boundary roughness of the FCF's mortar finish was defined by Ackers (1989) in terms of a Darcy–Weisbach friction factor as a function of the area mean Reynolds number:

$$\frac{1}{\sqrt{f}} = 2.02 \log\left(\mathrm{Re}\sqrt{f}\right) - 1.38 \qquad (1)$$

This formula represents the skin friction for boundary roughness without compound channel effects and was derived from tests conducted on a 'simple' non-compound channel of bed width 1.5 m and with side slopes of 2:1 (horizontal/vertical). From this, Ackers derived the best fit Manning's friction coefficient with flow depth for the facility ($n = 0.01\ \mathrm{m}^{1/3}\ \mathrm{s}^{-1}$). Hence, in the numerical simulations reported here a constant value of $n = 0.01\ \mathrm{m}^{1/3}\ \mathrm{s}^{-1}$ was used throughout the domain for all flow conditions. No roughness calibration was carried out. It may still be impossible to disaggregate error from other sources such as discretization errors (false diffusion), structural errors or errors of spatial resolution. However, the use of the FCF data means that errors arising from input data (flow boundary conditions, geometry) are reduced and the necessity for the calibration of skin friction is eliminated. Thus, the FCF experimental measurements provide a platform on which to conduct a robust validation for numerical models.

3. Numerical model description

The 2D finite element model TELEMAC-2D (Hervouet, 1989, 1993) was selected as the basis for the numerical simulations reported in this paper. This code has recently been extended to consider flood inundation applications by the incorporation of two specific developments. First, an algorithm was implemented to account for the effect of partially wet elements on the solution. Second, a Streamline Upwind/Petrov-Galerkin (SUPG) numerical method (Brooks and Hughes, 1982) was implemented to solve the combined propagation and diffusion step. This method is an improvement over classical upwind schemes in that it reduces the amount of numerical or 'false' diffusion and overcomes numerical oscillations associated with central-difference schemes in the solution of convection-dominated fluid flows. The method of characteristics is used to solve the advection step in the solution procedure.

The TELEMAC-2D code solves the 2D Shallow Water equations (also known as the Saint–Venant equations). These equations are obtained by means of averaging the full 3D Reynold's averaged Navier–Stokes equations for turbulent flow over the water depth. The resulting depth-averaged equations read: Continuity:

$$\frac{\partial h}{\partial t} + \overrightarrow{u}\cdot\overrightarrow{\mathrm{grad}}(h) + h\,\mathrm{div}(\overrightarrow{u}) = 0 \qquad (2)$$

x-momentum equation:

$$\frac{\partial u}{\partial t} + \overrightarrow{u}\overrightarrow{\mathrm{grad}u} = -\mathrm{g}\frac{\partial \mathrm{Z}}{\partial \mathrm{x}} + \mathrm{F_x} + \frac{1}{\mathrm{h}}\,\mathrm{div}\left(\mathrm{h}(\nu_\mathrm{T} + \mu)\overrightarrow{\mathrm{grad}u}\right) \qquad (3)$$

y-momentum equation:

$$\frac{\partial v}{\partial t} + \overrightarrow{u}\overrightarrow{\text{grad}v} = -g\frac{\partial Z}{\partial y} + F_Y + \frac{1}{h}\,\text{div}\left(h(\nu_T + \mu)\overrightarrow{\text{grad}v}\right) \quad (4)$$

The F_x and F_y source terms represent the force induced by boundary friction, whereby the depth-averaged volume force in terms of Mannning coefficient n, is given by: x-direction:

$$F_x = -\frac{1}{\cos\theta}\frac{g}{h^{4/3}n^2}u\sqrt{u^2+v^2} \quad (5)$$

y-direction:

$$F_y = -\frac{1}{\cos\theta}\frac{g}{h^{4/3}n^2}v\sqrt{u^2+v^2} \quad (6)$$

The Boussinesq approximation is used to model the Reynolds stress term that expresses the Reynolds stress as a function of the velocity gradients and a turbulent eddy viscosity. The normal stress term is ignored by TELEMAC-2D and in tensor notation is given below for $i \neq j$.

$$\overline{u_i u_j} = \rho\nu_T\left(\frac{\partial U_i}{\partial x_j} + \frac{\partial U_j}{\partial x_i}\right) \quad (7)$$

where the three components of the vector in a cartesian system (Fig. 3) are obtained by setting the index equal to 1, 2, 3, respectively.

Within the numerical framework provided by TELEMAC-2D, three turbulence closures schemes were tested: a constant viscosity model, the Elder formulae (Fischer et al., 1979) and the k–ϵ model. Simulations reported in this paper use all three of these turbulence models. For the constant eddy viscosity model, a single value of the parameter, ν_T, was specified throughout the domain and since this is usually an unknown value, this may form part of the calibration procedure or can be parameterized on the basis of physically based algebraic formulae. The Elder model employs dimensionless dispersion coefficients that are specified for the transverse (y) and longitudinal (x) directions so that the turbulent diffusion coefficients can be given by:

$$E_y = \alpha_y h u_* \quad (8)$$

$$E_x = \alpha_x h u_* \quad (9)$$

The turbulent diffusion coefficients for each direction are then substituted into their respective momentum equations in the place of the turbulent eddy viscosity. Again calibration may be undertaken for this model or it may be parameterized in a similar manner to the zero equation model. The k–ϵ model describes the turbulent eddy viscosity as a function of the turbulent kinetic energy (k) and the rate of its dissipation (ϵ):

$$\nu_T = c_\mu\frac{k^2}{\epsilon} \quad (10)$$

The transport equations for the turbulent kinetic energy and its dissipation rate are an extension of the classical model which was originally developed by Launder and Spalding (1974). The full set of the k–ϵ model equations reads:

$$\frac{\partial k}{\partial t} + \bar{U}_i\frac{\partial k}{\partial x_i} = \frac{\partial}{\partial x_i}\left(\frac{\nu_T}{\sigma_k}\frac{\partial k}{\partial x_i}\right) + P - \epsilon \quad (11)$$

$$\frac{\partial \epsilon}{\partial t} + \bar{U}_i\frac{\partial \epsilon}{\partial x_i} = \frac{\partial \epsilon}{\partial x_i}\left(\frac{\nu_T}{\sigma_k}\frac{\partial \epsilon}{\partial x_i}\right) + \frac{\epsilon}{k}(c_{1\epsilon}P - c_{2\epsilon}\epsilon) \quad (12)$$

where P is the production of turbulent kinetic energy by shear:

$$P = \acute{\imath}_T\left(\frac{\partial \bar{U}_i}{\partial x_j} + \frac{\partial \bar{U}_j}{\partial x_i}\right)\frac{\partial \bar{U}_i}{\partial x_j} \quad (13)$$

The standard k–ϵ turbulence model was developed to describe a flow field in three dimensions however Rastogi and Rodi (1978) developed a depth-averaged form which has been implemented within TELEMAC-2D. Here, the above equations are solved with the modification that the vertical-averaging procedure gives rise to a further production term in both transport equations due to bed shear stress (for a full description see Rodi, 1980 or Hervouet and Van Haren, 1994). The k–ϵ transport equations have standard constants for a variety of flow applications and the values associated with free-surface flow with no imposed obstructions, are used within the TELEMAC-2D code (see Rodi, 1980). This means that a turbulence parameter calibration is not necessary for each separate case with this closure model.

4. Numerical simulations

Finite element meshes were configured on an identical scale to the series A and series B physical models (see Fig. 2a and b). The series A mesh contains approximately 4500 elements and 2300 computational nodes, whilst the series B mesh contains approximately 3700 elements and 2000 computational nodes. Both discretizations were constructed to be typical of those used for reach-scale flood modeling studies (see Gee et al., 1990; Feldhaus et al., 1992; Bates et al., 1998) and have approximately the same computational burden. Thus, conclusions drawn regarding the suitability of the method for within reach stage-discharge prediction are potentially transferable to field applications. Choice of mesh resolution and topology for such studies is still fundamentally limited by available computing power. With TELEMAC-2D, the maximum number of nodal points that can be solved even on a high power workstation is of the order 10–30,000. For practical studies, a maximum number an order of magnitude less is more realistic given typical time constraints. To achieve a discretization of a channel-floodplain reach using this number of nodes requires a number of compromises. Whilst numerical schemes typically operate best with regular elements (equilateral triangles in this case) and smooth gradations between small and large elements, this optimum needs to be relaxed in order to facilitate reach-scale studies. A typical solution elongates the channel elements (in our case triangles) in the downstream direction by a ratio between 4:1 and 5:1 (see Bates et al., 1998). This ratio is a rule of thumb based on experience and a limited number of comparative tests (Bates et al., 1995). Elongation of channel elements also reduces the resolution at which near-channel parts of the floodplain are represented. The reasoning here is that, despite the presence of gradient and divergence terms in the controlling equations, the down reach velocity gradients will be small compared to the lateral velocity gradient and given the understanding of compound channel flow mechanisms detailed above it may be more important to concentrate detail on adequately resolving the eddies created at the channel–floodplain interface. Yet even so the channel cross section can still only be represented with 3–5 nodes if we wish to retain sufficient nodes to represent potentially complex floodplain topography given finite computational resources. Such floodplain resolution is often required as a primary use of reach-scale models is for inundation extent prediction. Moreover, the greater complexity of the floodplain discretization in the meandering channel case means that fewer element are available to discretize the channel and this is consequently of a coarser resolution. At present we do not know the mesh resolution at which lateral velocity profiles and floodplain–channel momentum exchange need to be represented to achieve different application objectives, such as stage, velocity and inundation extent prediction. Thus, typical mesh generation rules may still result in a relatively coarse lateral discretization of the channel–floodplain interface and hence a subsidiary aim of the research reported here was to test established ideas regarding mesh generation for floodplain modeling against a benchmark data set.

Parameters for the model simulations consisted of a single Manning coefficient, a value for the eddy viscosity coefficient, v_T, in the case of the zero equation turbulence closure and values for the dimensionless coefficients E_x and E_y in the case of the Elder model. As noted above the Manning coefficient was set to 0.01 $m^{1/3}\ s^{-1}$ for all simulations on the basis of results reported by Ackers (1989), whilst v_T for the constant eddy viscosity model was calculated using a physically based algebraic formulae. In situations where the prescribed diffusion is significantly greater than the physical diffusion, the model predictions will be over-diffused and distorted compared to the observed data. In the simulations reported in this paper a value of v_T was calculated from the formula given by Keefer (1971):

$$v_T = \beta h u_* \tag{14}$$

From an experimental investigation involving a flume of rectangular cross-section, Keefer proposed a value of 0.11 for the dispersion coefficient β. However, for asymmetric compound channel flow, the depth-averaged transverse dispersion coefficient has been found to be higher and greater than 0.13 (Wood and Liang, 1990). Furthermore, Jenkins (1993) found that the value of the depth-averaged dispersion coefficient is distinctly higher in a symmetrical channel, where $\beta = 0.27$, than in an asymmetric channel $\beta = 0.06$. This higher value corresponds to values of v_T in the range

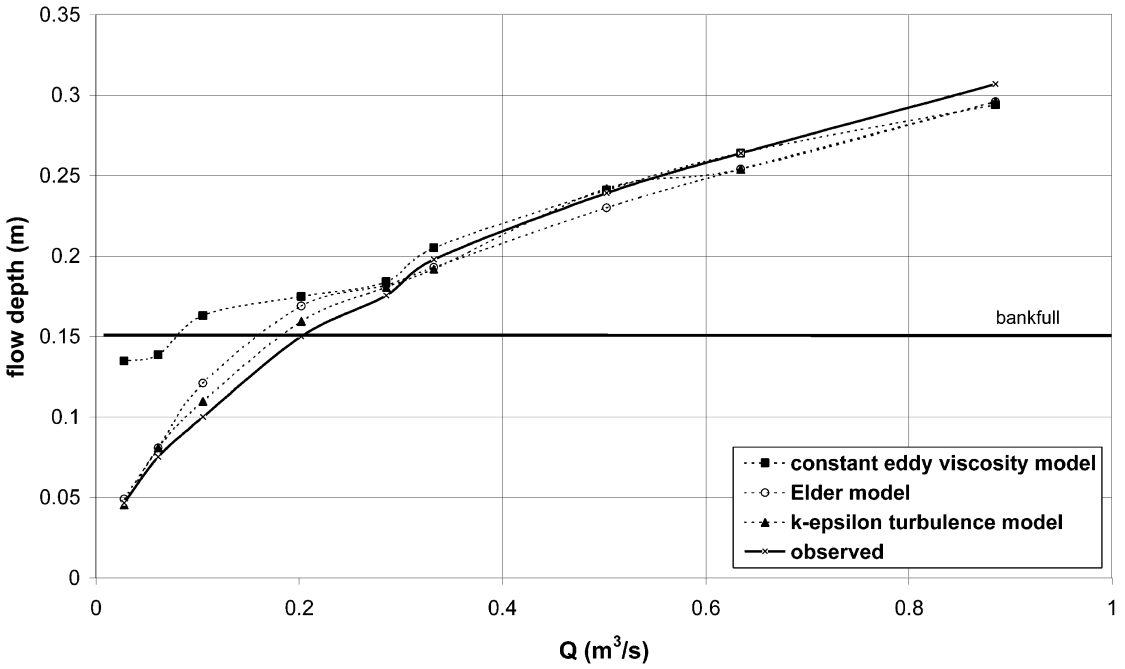

Fig. 4. Comparison of the observed stage-discharge rating curve for the series A configuration with the predicted values by the different turbulence models.

10^{-4}–10^{-3} $m^2\,s^{-1}$ for the flow conditions examined in this paper.

It should be noted that previously reported values for v_T used in numerical simulations are typically in the range 0.1–2.0 $m^2\,s^{-1}$ (see Bates et al., 1998). The lower values used here in the simulations reported in this paper (10^{-4}–10^{-3} $m^2\,s^{-1}$) should introduce less artificial diffusion and hence lead to a greater degree of physical realism in the simulations. In the case of the Elder model, Moulin (1995) has undertaken comprehensive sensitivity tests for the transverse and longitudinal dimensionless dispersion coefficients used in this scheme. The values resulting from the Moulin study ($\alpha_x = 6.0$ $\alpha_y = 0.6$) were thus used in the Elder model simulations reported here. It should be noted that ideally these coefficients should be implemented using a channel-fitted co-ordinate system and their direction should vary as a function of channel curvature. This has not been attempted here, yet even for the fixed reference frame employed the sense of the transverse and longitudinal dispersion is still broadly maintained even in the most sinuous meandering case.

The FCF physical model was run to uniform flow for a series of fixed (steady state) discharges, which taken together allow construction of stage-discharge rating curves for each configuration for the transition from inbank to overbank flow conditions. Hence, each run corresponded to a different point on the rating curve. The boundary conditions used in the simulations consisted of a fixed upstream discharge and a fixed downstream flow depth. All other boundaries were specified as impermeable with a slip condition. Finally, the precision of the numerical solver was set to an accuracy of 1×10^{-8} for all simulations. Errors in the mass balance were less than 0.05% for all turbulence models based on runs of 2000 time steps, although convergence rates varied both for inbank and overbank flow conditions. Convergence was attained when the predicted discharge was within 0.1% of the prescribed discharge. The model was run until steady-state uniform conditions were achieved. This occurred when all waves or oscillations had faded out of the system, and the water depths and velocities were constant in time and space. In practice, configuration of the inlet boundary will

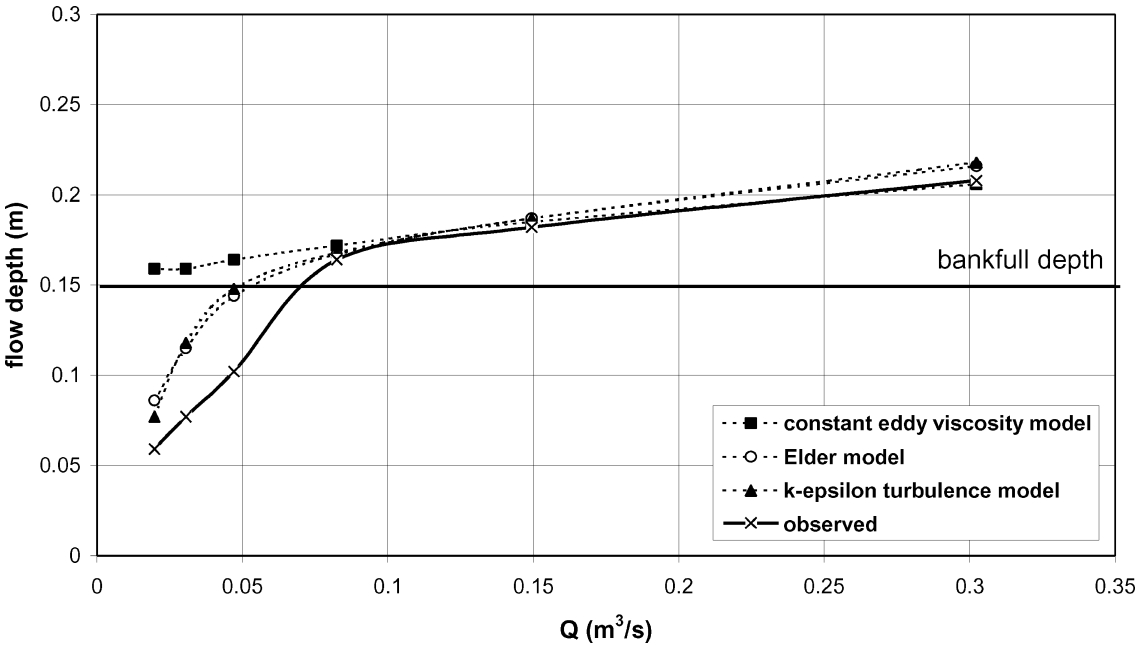

Fig. 5. Comparison of the observed stage-discharge rating curve for the series B configuration with the predicted values by the different turbulence models.

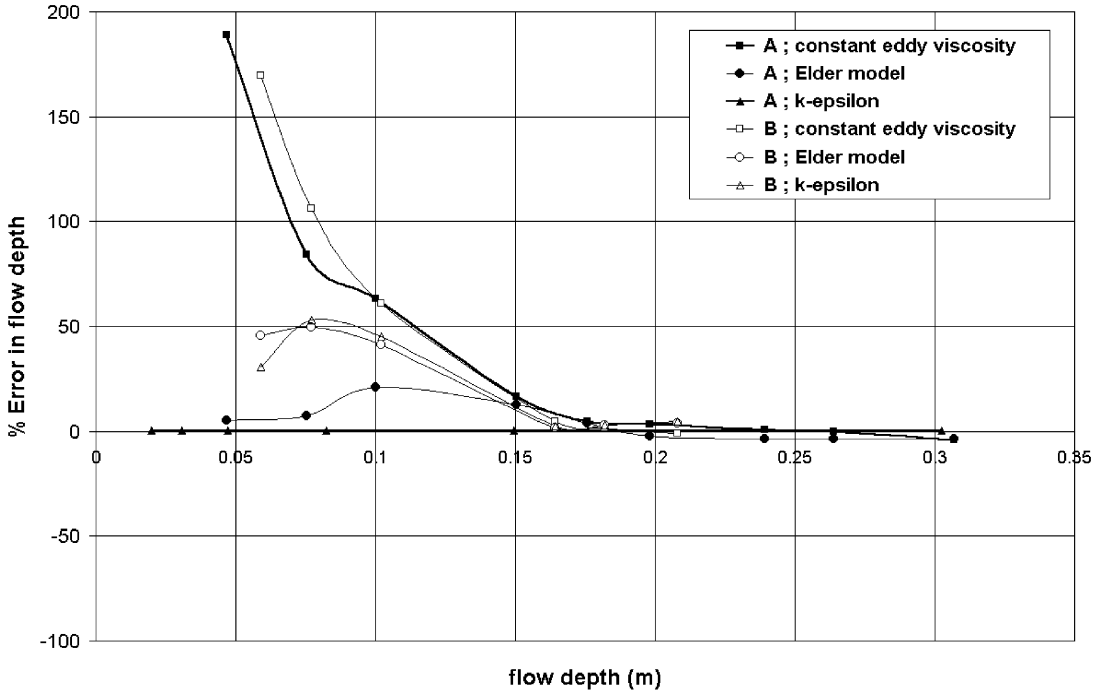

Fig. 6. Percentage error in computed flow depth for all turbulence models for straight and meandering channel configuration; bankfull flow depth is 0.15 m.

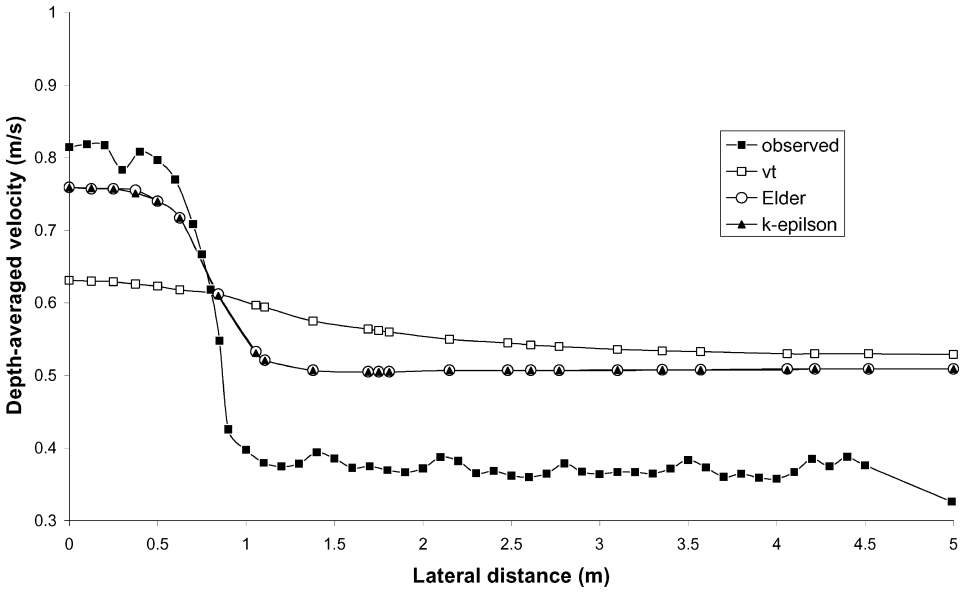

Fig. 7. Lateral distribution of the depth-averaged velocity for a flow depth of 200 mm (DR = 0.333) for the series A channel.

mean that uniform conditions will only occur at some distance from this boundary once the flow has had time to fully establish. With this proviso, model results and experimental data should be comparable.

The simulation results from the three turbulence models were compared in terms of their ability to reproduce measured stage-discharge points. This was investigated further by comparing the computed depth-averaged velocity distributions with those observed in the experimental programme. In the case of the straight channel (A) this was taken at a point half way along the physical model and for the meandering channel case (B), a cross section on one of the bends was selected. The numerical model's predicted flow depths were reach-averaged.

5. Results and discussion

Both in the straight (A) and meandering (B) compound channel cases, when modeling the mean flow parameters, the Elder and $k-\epsilon$ turbulence models show a definite improvement for the modeling of inbank and low overbank flow conditions (see Figs. 4–6) over the constant eddy viscosity model. In the case of the straight channel for inbank flows the $k-\epsilon$ representation of turbulence gives marginally better predictions than the Elder model, whilst at the lowest flow depth examined both turbulence models can predict flow depth to an accuracy of 5%. By contrast, the constant eddy viscosity model over-estimated flow depth by a maximum of 190%. For the meandering channel case, the Elder and $k-\epsilon$ turbulence model flow depth predictions again show a very similar degree of error for inbank and low overbank flows, and are a definite improvement over the constant eddy viscosity model. However, the prediction accuracy of the Elder and $k-\epsilon$ models is not as great as in the straight channel case, where the flow has relatively weaker secondary currents relative to the meandering channel situation and the mesh resolution is coarser. For meandering channels, the Elder and $k-\epsilon$ models still improve the stage prediction at the lowest inbank flows from an over-estimation of 170% by the constant eddy viscosity model to an overestimation of 25–45%. However for moderate overbank flow conditions, where the relative depth defined as:

$$\mathrm{DR} = h_f/y_{bk} \tag{15}$$

where h_f is the depth of floodplain flow and y_{bk} is the bankfull depth, is ≥ 0.5, all turbulence models predict flow depth to a very similar degree of error (5%) for the straight and meandering channel configurations.

Comparison of the observed and computed

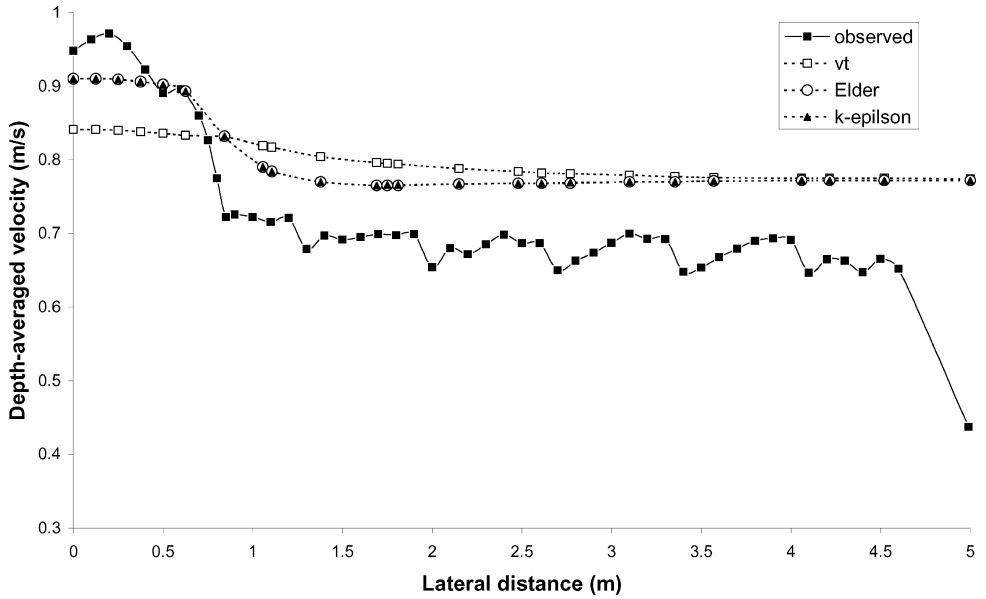

Fig. 8. Lateral distribution of the depth-averaged velocity for a flow depth of 250 mm (DR = 0.666) for the series A channel.

depth-averaged velocity distributions were made in the region of the main channel and at the main channel–floodplain interface (at the time of writing floodplain velocity measurements were not widely available). The depth-averaged velocity distribution was examined for the straight and meandering configurations at a low to medium overbank flow depth ($h = 200$ mm, DR = 0.333) and a high overbank flow depth ($h = 250$ mm, DR = 0.666), see Figs. 7–10. These correspond to flow conditions at which

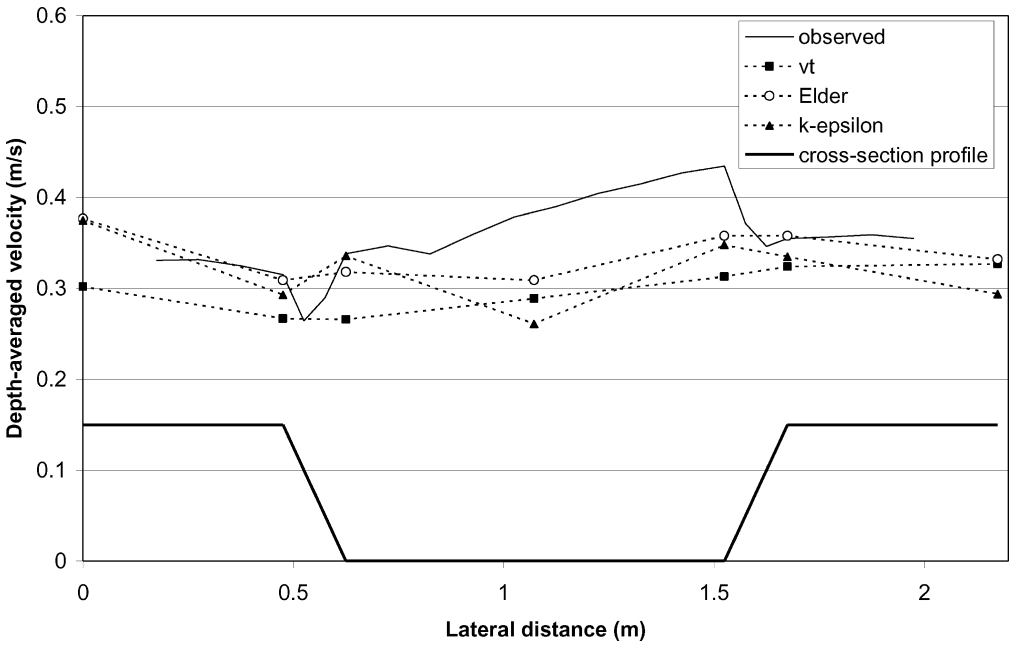

Fig. 9. Lateral distribution of the depth-averaged velocity for a flow depth of 200 mm (DR = 0.333) for the series B channel.

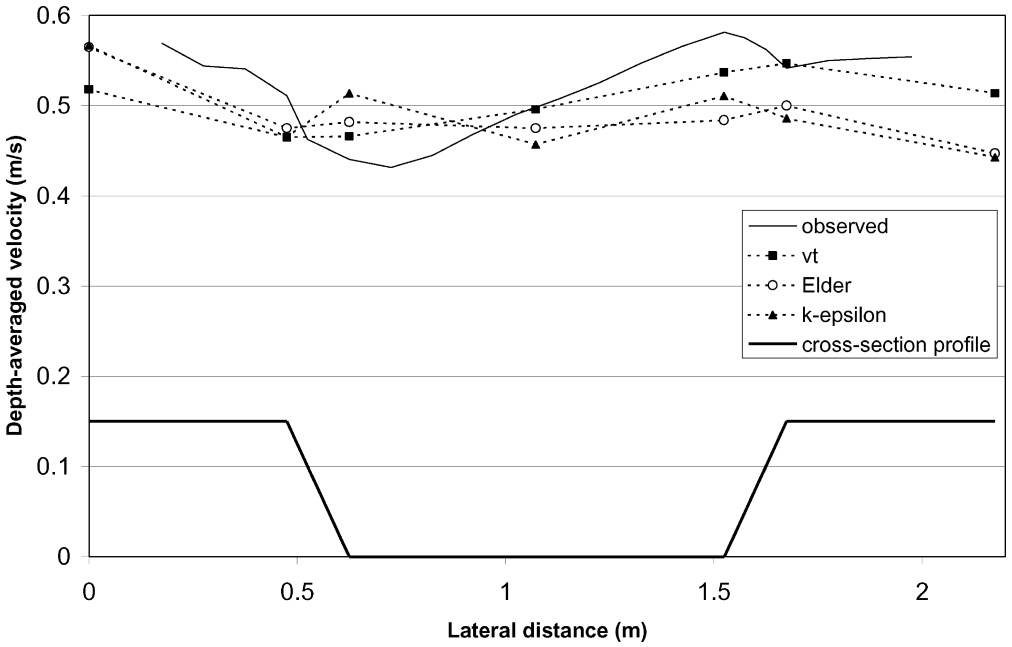

Fig. 10. Lateral distribution of the depth-averaged velocity for a flow depth of 250 mm (DR = 0.666) for the series B channel.

velocity measurements were made in the experimental programme.

In the series A programme, it was observed that the difference in main channel and floodplain zonal velocities promoted the formation of a bank of vortices with vertical axes along the main channel–floodplain interface and hence the development of a horizontal shear layer. A steep gradient in depth-averaged velocity distribution in this vicinity is associated with this flow mechanism that is more emphasized at the lower relative depth (Figs. 7 and 8). In particular, there is a rather odd but regular 'dip' in velocity on the floodplain that is probably related to how the channel was roughened and which may not be accounted for in the uniform skin friction value calculated by Ackers (1989). It may be that at this point that the roughness exerts a greater control over the flow field than turbulence (see Lane and Richards, 1998 for a demonstration of this in a simpler 2D model). Given our approach to friction parameterization this may be difficult to pick up in any of the models, and in particular the constant eddy viscosity model fails to predict the large change in depth-averaged velocity between the main channel and floodplain zones at both flow depths. For this turbulence closure at the lower relative depth there are errors in the computed velocity of up to 55% compared to errors of up to 25% at the higher depth. The Elder and $k-\epsilon$ models capture the change in depth-averaged velocity distribution between the two channel zones with better accuracy for both flow depths, but there is still under-estimation of the main channel flow and over-estimation of the floodplain flows. This corresponds well with the relative performance of these turbulence models in terms of stage-discharge prediction. Explanations may include a failure to account for secondary flows in the TELEMAC-2D model which has been noted by Shiono and Knight (1991) to contribute significantly to apparent shear stress at the channel–floodplain interface or poor grid resolution in this region in reach-scale model discretizations.

In the meandering channel case, comparisons between the observed and computed lateral distribution of depth-averaged velocity were made for a single cross-section located on the bend (Figs. 9 and 10). Here again, all turbulence models had greater errors in computed velocity at the lower depth (up to 25% error), than at the higher depth (up to 17% error). Whilst there may be problems with the roughness parameterization, a further problem with replicating

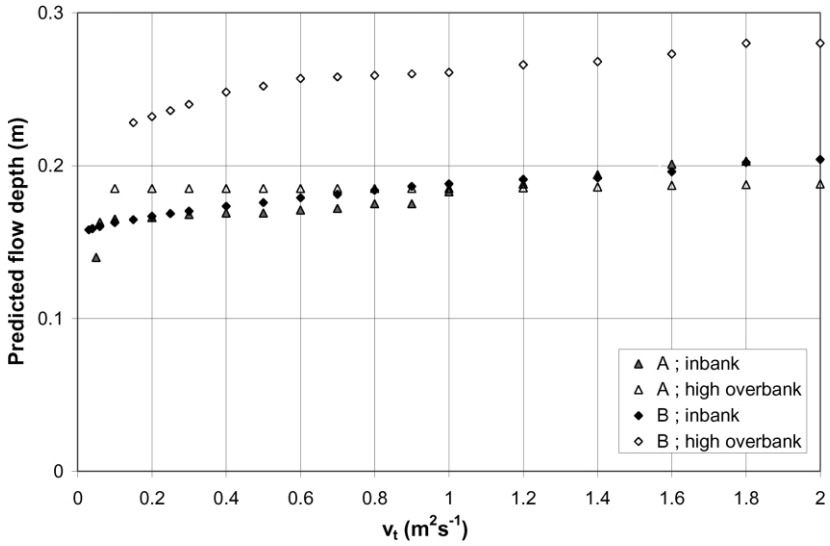

Fig. 11. Variation in predicted flow depth with turbulent eddy viscosity for the series A and series B channels for inbank and overbank flow conditions (using the constant eddy viscosity model).

these velocity profiles is the fact that the measured velocity gradients are steep compared to the relatively coarse mesh resolution used to represent them. In effect, the model is unable to resolve the lateral velocity gradient because of the coarse discretization. Whilst higher order turbulence closures suffer less in this respect, their ability is fundamentally constrained by the mesh properties. This has important implications for the mesh discretization strategies typically used in the simulation of compound channel hydraulics at the reach-scale.

All turbulence models produce better results for overbank flows than inbank flows (see Fig. 6). This is likely to be due to a combination of the coarse mesh resolution in the main channel and the fact that for compound channel discretizations at low in bank flow partially wet elements occur on the steep (45°) channel side slopes. This may generate spurious water surface slopes that are difficult to correct (see Bates et al., 1998) and lead to poor prediction of velocity vectors. However, for overbank flows all elements are fully wet and this problem does not arise. Such steep slopes may also cause a conflict with one of the fundamental assumptions of the Shallow Water equations, namely that slopes be less than 10%. The exception to this rule is the k–ϵ model applied to the straight channel case which shows no bias in its performance between inbank and overbank flow conditions in its performance. However as explained in Section II, this is a much simpler flow situation that is more hydraulically 2D than the meandering channel case and one might expect reasonable prediction of the stage-discharge relationship with a 2D model. It is interesting to note that the constant eddy viscosity model has its poorest predictive ability at the lowest flow depth (this is also the case for the Elder model when applied to the meandering channel case) when the greatest number of dry cells exists within the domain. The difficulty of modeling accurately domains which contain some dry cells has also been experienced by Olsen and Wilson (1999) using the 3D finite volume code SSIIM.

The sensitivity of the turbulent eddy viscosity (ν_T) with respect to the model's predictive ability was assessed for both straight and meandering configurations. Analysis was conducted for both an inbank and overbank stage-discharge point (at similar h/y_{bf} ratios) for values of the parameter ν_T in the range 0.05–2.0 $m^2 s^{-1}$. It should be noted that these values are more in line with those used in previous studies (Bates et al., 1998).

Increasing the turbulent eddy viscosity introduces artificial diffusion to the predicted flow field and results in an increase in free surface elevation (see

Fig. 11). However, one should be aware that this parameter has a potentially complex relationship with grid size. For the inbank flow condition, with the exception of simulations conducted with v_T less than 0.1, increasing the parameter v_T resulted in an increase in the computed flow depth. A similar degree of flow depth increase was experienced for both the straight (A) and meandering (B) channel configurations. This corresponds to an increase in percentage error in flow depth prediction ranging from approximately 75–100% (at minimum v_T values) up to 165–170% (at higher v_T values) where the percentage error is defined as:

$$\text{Prediction Error} = 100 \times \frac{h_{\text{computed}} - h_{\text{observed}}}{h_{\text{observed}}} \quad (16)$$

However for the overbank flow condition, there is a difference in the manner by which the predicted flow depth varies with the parameter v_T for the straight and meandering channel cases. The percentage error in predicted flow depth varies in the range from 5 to 7% with increasing v_T for the straight channel, whilst for the meandering channel the error in predicted flow depth varies in the range 10–34%. This has important implications in flood routing, as in practice artificial diffusion is often added to improve numerical stability.

6. Conclusions

The simulations reported in this paper demonstrate that for typical reach-scale mesh discretizations, a two dimensional finite element model, regardless of turbulence closure used, is an adequate predictor of the stage-discharge rating curve for moderate and high overbank flow conditions. However the Elder and k–ϵ turbulence models can reproduce inbank and low overbank stage-discharge points with better accuracy than the constant eddy viscosity model for both straight and meandering channels. Here, the k–ϵ model can predict hydraulic variables with marginally better accuracy than the Elder model for the straight channel case, and by a similar accuracy for the meandering channel case. However, for overbank flows all models have similar predictive ability. The computed lateral depth-averaged velocity distribution for the discretizations tested here was predicted relatively poorly for all turbulence models, with the higher order turbulence model performing marginally better then than simplest zero-equation models. This is likely to be a consequence of the coarse mesh resolution in near channel areas typically necessary to facilitate reach-scale studies using two dimensional finite element techniques. This was insufficient to allow the model to replicate the observed steep velocity gradients observed in this region and hence resulted in poor process representation. The sensitivity of the turbulence parameter calibration with respect to the predicted flow depth has also been addressed for the constant eddy viscosity model and shows that although higher accuracy (at high overbank flows) can be achieved using a constant eddy viscosity model this is highly dependent on the particular value selected. This highlights an additional advantage of the k–ϵ turbulence model.

In relation to reach-scale studies, we can conclude that a depth-averaged model with k–ϵ turbulence closure can, when used with a relatively coarse mesh discretization, adequately predict the stage-discharge rating curve for a given intermediate cross section based on non-local boundary conditions. For overbank flows the even simpler zero equation model will suffice. Such schemes are theoretically adequate predictors of flood inundation extent as this merely requires a model capable of replicating water surface elevations at cross sections along a reach during overbank conditions as long as the model incorporates sufficiently accurate floodplain topographic information at the required scale. The results for the k–ϵ model also show that the lateral velocity profile needs only to be relatively crudely approximated to predict water depth correctly from the inbank to overbank transition. Where a model is required to predict lateral velocity profiles, rather than free surface elevations, a much more finely resolved discretization of the near channel zone than those used here might potentially be required. Three-dimensional and secondary current effects may also become important for velocity prediction, particularly in the case of meandering channels, although the evidence presented here does not rule out the possibility that a more finely resolved 2D code would be sufficient. Further validation of these turbulence models against field scale data needs to be conducted in order to confirm the optimum turbulence model for different

categories of flow problems so that CFD codes can be used as robust engineering tools.

Acknowledgements

This research was supported by EPSRC Grant GR/L 95694. We wish to thank all research, students, staff and academics who took part in both the FCF series A and B experiments in particular those who helped to collect the data which is used in this paper; and both reviewers for providing constructive and helpful editorial comments.

References

Ackers, P., 1989. Resistance functions for the Wallingford Facility, SERC Flood Channel Research Design Manual Technical Report No. 1, August.

Alavian, V., Chu, V., 1985. Turbulent exchange flow in shallow compound channel. Proceedings of the 21st Congress of the IAHR, Melbourn, Australia, pp. 447–451.

Arnold, U., Hötges, J., Rouvé, G., 1989. Turbulence and mixing mechanisms in compound open channel flow. Proceedings of the 23rd Congress of the IAHR, Ottawa, Canada, pp. 21–28.

Bates, P.D., Anderson, M.G., Hervouet, J.-M., 1995. An initial comparison of two 2-dimensional finite element codes for river flood simulation. Proceedings of the Institution of Civil Engineers, Water, Maritime and Energy, 112, pp. 238–248.

Bates, P.D., Stewart, M.D., Siggers, G.B., Smith, C.N., Hervouet, J.-M., Sellin, R.H.J., 1998. Internal and external validation of a two dimensional finite element model for river flood simulation. Proceedings of the Institution of Civil Engineers, Water Maritime and Energy, 130, pp. 127–141.

Brooks, A.N., Hughes, T.J.R., 1982. Streamline Upwind/Petrov Galerkin formulations for convection dominated flows with particular emphasis on the incompressible Navier–Stokes equations. Computer Methods in Applied Mechanics and Engineering 32, 199–259.

Cokljat, D., Kralj, C., 1997. The choice of turbulence model for prediction of flows over river bed forms. Journal of Hydraulic Research 35 (3), 355–361.

Feldhaus, R., Höttges, J., Brockhaus, T., Rouvé, G., 1992. Finite element simulation of flow and pollution transport applied to a part of the River Rhine. In: Falconer, R.A., Shiono, K., Matthews, R.G.S. (Eds.). Hydraulic and Environmental Modelling; Estuarine and River Waters. Ashgate Publishing, Aldershot, pp. 323–344.

Fischer, H.B., List, E.J., Koh, R.C.Y., Imberger, J., Brooks, N.H., 1979. Mixing in Inland and Coastal Waters. Academic Press, San Diego.

Gee, D.M., Anderson, M.G., Baird, L., 1990. Large scale floodplain modelling. Earth Surface Processes and Landforms 15, 513–523.

Greenhill, R.K., 1992. An Investigation into the Mechanisms of Compound Channel Flow, PhD Thesis, Department of Civil Engineering, University of Bristol, UK.

Greenhill, R.K., Sellin, R.H.J., 1993. Development of a simple method to predict discharges in compound meandering channels. Proceedings of Institute of Civil Engineers, Water Maritime and Energy, London, 101, pp. 37–44.

Hervouet, J-M., 1989. Comparison of experimental data and laser measurements with computational results of the TELEMAC-2D code (Shallow Water equations. In: Maksimovic, C., Radojkovic, M. (Eds.). Computational Modelling and Experimental Methods in Hydraulics (HYDROCOMP'89). Elsevier, Amsterdam.

Hervouet, J-M., 1993. Validating the numerical simulations of dam-breaks and floods. Proceedings of an International Conference on Hydroscience and Engineering, Washington, pp. 754–761.

Hervouet, J-M., Van Haren, L., 1994. TELEMAC-2d Version 3.0 Principle Note, EDF Electricite de France, Departement Laboratoire National d'Hydraulique.

Jenkins, G., 1993. Estimating eddy kinematic viscosity in compound channels. In: Wang, S. (Ed.). Advances in Hydro-Science and Engineering 1(B). , pp. 1277–1282.

Keefer, T.N., 1971. The Relation of Turbulence to Diffusion in Open Channel Flows, PhD Thesis, Department of Civil Engineering, Colorado State University.

Knight, D.W., 1999. Flow mechanisms and sediment transport in compound channels. International Journal of Sediment Research 14 (2), 217–236.

Knight, D.W., Shiono, K., 1990. Turbulence measurements in a shear layer of compound channel. Journal of Hydraulic Research 28 (2), 175–196.

Lane, S.N., Richards, K.S., 1998. High resolution, two-dimensional spatial modelling of flow processes in a multi-thread channel. Hydrological Processes 12 (8), 1279–1298.

Launder, B.E., Spalding, D.B., 1974. The numerical computation of turbulent flows. Computer Methods in Applied Mechanics and Engineering 3, 269–289.

Lin, B., Shiono, K., 1995. Numerical Modelling of solute transport in compound channel flows. Journal of Hydraulic Research 33 (6), 773–787.

Miller, A.C., 1971. Turbulent Diffusion and Longitudinal Dispersion Measurements in a Hydrodynamically Rough Open Channel Flow, PhD Thesis, Department of Civil Engineering, Colorado State University.

Moulin, C., 1995. Anisotropie de la Dispersion pour le Transport Bidimensional dans le Systeme TELEMAC, EDF Internal Report, HE-43/95/016/A, Department Laboratoire National d'Hydraulique, EDF Chatou, Paris.

Naot, D., Nezu, I., Nakagawa, H., 1993. Calculation of compound open channel flow. ASCE Journal of Hydraulic Engineering 119 (12), 1418–1426.

Olsen, N.R.B., Wilson, C.A.M.E., 1999. CFD modelling of rivers and reservoirs. Proceedings of the Optimum Use of Hydropower Schemes, International Centre for Hydropower, Trondheim, Norway, June.

Rastogi, A.-K., Rodi, W., 1978. Predictions of heat and mass transfer in open channels. Journal of Hydraulics Division, ASCE HY3, 397–420.

Rodi, W., 1980. Turbulence models and their application in hydraulics, IAHR State-of-the-art Review, Delft, IAHR.

Samuel, P.G., 1985. Modelling of river and flood plain flow using the finite element method. Hydraulics Research Ltd Wallingford, Technical Report. SR61

Sellin, R.H.J., 1961. A Study of the Interaction between the Flow in the Channel of a River and that over its Flood Plain, PhD Thesis, Department of Civil Engineering, University of Bristol, UK.

Shiono, K., Knight, D.W., 1991. Turbulent open channel flows with variable depth across the channel. Journal of Fluid Mechanics 222, 617–646.

Shiono, K., Muto, Y., 1998. Complex flow mechanisms in compound meandering compound channels with overbank flow, . Journal of Fluid Mechanics, Cambridge, UK 376, 221–261.

Shiono, K., Al-Romaih, J.S., Knight, D.W., 1999. Stage-discharge assessment in compound meandering channels. ASCE Journal of Hydraulic Engineering 125 (1), 66–77.

Wark, J.B., James, C.S., Ackers, P., 1994. Design of straight and meandering compound channels, National Rivers Authority, R and D Report 13, 1992, National Rivers Authority, Bristol, UK.

Willetts, B.B., Hardwick, R.I., 1993. Stage dependancy for overbank flow in meandering channels. Proceedings of Institute of Civil Engineers, Water Maritime and Energy, 101, pp. 45–54.

Wilson, C.A.M.E., 1999. The effect of floodway width on the conveyance capacity in a scale model of the series B, IAHR 28th Conference Congress, Graz, Austria, August.

Wood, I.R., Liang, T., 1990. Dispersion in an open channel with a step in the cross-section. Journal of Hydraulic Research IAHR 27 (5), 587–601.